Deep-Sea Research II 118 (2015) 250–260

Contents lists available at ScienceDirect

Deep-Sea Research II

journal homepage: www.elsevier.com/locate/dsr2

Oceanic pCO_2 in the Indian sector of the Southern Ocean during the austral summer–winter transition phase

Suhas S. Shetye [a,b,*], Rahul Mohan [b], Shramik Patil [b], Babula Jena [b], Racheal Chacko [b], Jenson V. George [b], Sharon Noronha [b], Neelu Singh [b], Lakshmi Priya [a], Maruthadu Sudhakar [c]

[a] National Institute of Oceanography, Dona paula, Goa 403004, India
[b] National Centre for Antarctic & Ocean Research, Headland Sada, Goa 403804, India
[c] Ministry of Earth Sciences, New Delhi 110003, India

ARTICLE INFO

Available online 12 June 2015

Keywords:
Southern Ocean
Fronts
Primary production
Redfield ratio

ABSTRACT

Biogeochemical processes in the Southern Ocean (SO) play a significant role in regulating the global climate. The physical and biological processes controlling pCO_2 in the surface mixed layer at the Indian sector of SO were observed, and changes during the transition period from summer to early winter (January, February and March) were compared. An existing, one-dimensional model describing the mixed-layer carbon cycle was used to determine the relative contributions of biological activity, mixing, thermal and air–sea fluxes on pCO_2. A breakdown of the controls shows that the pCO_2 distributions are dominated by biological processes during January and February, whereas mixing and thermal effects contributed equally during March. Biological processes accounting for pCO_2 decrease reached a maximum value of 108 μatm during January. Our results are categorized according to distinct hydrographic regions such as oceanic fronts Sub-tropical front (STF), Sub-Antarctic front (SAF), Polar front (PF) and Antarctic zone (AZ). pCO_2 varied among these three studied months, the mean pCO_2 increasing from 286 μatm in January to 337 μatm in March, whereas an opposite trend was observed with dissolved oxygen (O_2). The satellite-derived Primary Production (PP) decreased from January to March and also from the STF towards the SAF, PF and AZ. The observed differences in PP and pCO_2 during the three months showed the total diatom count ranging from 0.49×10^3 cells/l in March to 3.2×10^3 cells/l in January. Our study indicates that the drawdown in sea-surface pCO_2 from March to January could be attributed to the light availability, shallow Mixed layer depth (MLD), high PP, nutrient availability, and low upwelling velocity. Eddies play an important role in regulating pCO_2 that require further studies to quantify their percentage contribution in pCO_2 rise/drawdown.

1. Introduction

The Southern Ocean (SO) has been predicted to be heavily impacted by climate change, by altering the surface water stratification (Sarmiento et al., 2004), reducing the vertical nutrient supply thereby hindering the phytoplankton growth (Bopp et al., 2001, 2005), and intensifying the mid-latitude Westerlies thus affecting the upwelling strength and MLD (Lenton and Matear, 2007). Recent studies have identified that the high latitude SO is a region where the oceanic pCO_2 growth rate is greater than that of the atmosphere (Metzl, 2009; Takahashi et al., 2009), implying that the strength of the oceanic CO_2 sink has decreased recently. Data collected from the south of 50°S during the summer showed that the pCO_2 is highly variable, with a mixture of various CO_2 sources and sinks the intensities and locations of which evolve with time (Metzl et al., 1991). Documenting and understanding the trends in oceanic pCO_2, dissolved oxygen and nutrients are important both from the perspective of global environmental change and for furthering our knowledge of biogeochemical processes.

Most earlier studies on pCO_2 focus on the mean rates of change in the oceanic uptake of atmospheric CO_2 and use the annual means of the partial pressure of CO_2 in seawater, assuming that its seasonal cycle remains unchanged (Takahashi et al., 2009; Schuster et al., 2009). However, in the SO, the seasonal cycle is known to be one of the strongest modes of variability that couples the physical mechanisms of climate forcing and ecosystem response in production, diversity and carbon export (Monteiro

* Corresponding author.
E-mail address: suhasshetye@gmail.com (S.S. Shetye).

http://dx.doi.org/10.1016/j.dsr2.2015.05.017
0967-0645/

et al., 2011). Louanchi et al. (1996) calculated breakup of different processes that could impact pCO_2 and showed that there were significant seasonal and inter-annual variations of the percentile contribution of different processes. Therefore, to obtain a greater understanding of processes controlling pCO_2, we have determined the dominant mechanisms that control the characteristics of surface pCO2 in the SO during the austral summer–winter transition phase.

2. Methodology

Research cruises were conducted in the Indian sector of the SO onboard R/V Akademik Boris Petrov, ORV Sagar Nidhi and Ivan Papanin during March 2009, February 2010 and January 2012, respectively (Fig. 1). Seawater samples were collected along two transects, marked in Fig. 1 as TW (30°S to 65°S along 48°E) and TE (30°S to 66°S along 57°30'E) during March 2009 and February 2010, and along 38–66°S and 20–76°E during January 2012. Samples were also collected from standard depths (0, 20, 40, 60, 80, 100, 120, 150, 200, 300, 400, 500, 600, 800, 1000 m) along the two transects using a Rosette sampler with 10 L capacity Niskin bottles mounted on the Conductivity–Temperature–Depth (CTD) assembly during March 2009 and February 2010. During January 2012, only surface water samples were collected.

Satellite-derived parameters such as upwelling velocity, sea surface temperature (SST), photosynthetically active radiation (PAR) and chlorophyll-*a* were used to understand the biogeochemical processes in the Indian Ocean sector of the SO.

2.1. Satellite-derived environmental parameters

2.1.1. Computation of upwelling velocity

The MetOp–ASCAT-measured Level-2 wind vectors were derived from Level-1b data, using a Geophysical Model Function (GMF), which relates normalized radar cross-section (σ0) to wind speed and direction (Hersbach et al., 2007). For our analysis, the scientific quality Level-2 daily swath data files available at 12.5 km wind vector cell (WVC) spacing were composited for valid data pixels to generate monthly images. Wind stress was calculated from the ASCAT Level-2 swath data using the Tropical Ocean Global Atmosphere—Coupled Ocean Atmosphere Response Experiment (TOGA–COARE) algorithm (Fairall et al., 1996). The curl was calculated using centered differences for the derivatives, based on gridded files of the individual orbits (Gill, 1982). Further, Ekman upwelling was computed as $(\mathrm{curl} \times \tau)/(\rho \times f)$ where, "τ" is the wind stress, "ρ" is the density of surface water and "f" is the Coriolis parameter (Pond and Pickard, 1983).

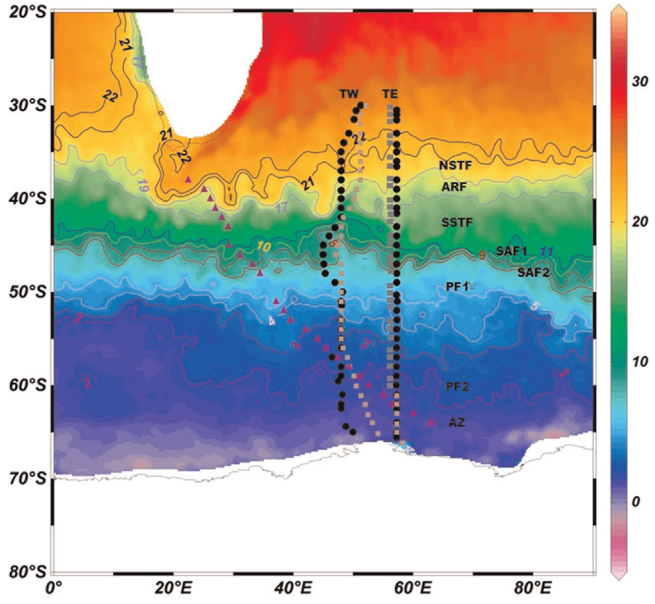

Fig. 1. Climatological AMSR-E Sea Surface Temperature for 2010. Fronts were marked following Anilkumar et al., 2006. Black circles, gray boxes and pink triangles denote sampling points during March 2009, February 2010 and January 2012, respectively. (For interpretation of the references to color in this figure legend, the reader is referred to the web version of this article.)

2.1.2. Photosynthetically active radiation (PAR)

An Aqua-MODIS-derived photosynthetically active radiation product is available in varied spatial (1 km to 1°) and temporal resolutions (up to yearly composite). We used a level-3 monthly composite product of PAR with a spatial resolution of 4.6 km. PAR is crucial for determining photosynthetic rate of phytoplankton growth and oceanic primary production. The irradiance model of Gregg and Carder (1990) used a mixture of marine and terrigenous aerosols and formed the basis for algorithm for the MODIS PAR product.

2.1.3. Chlorophyll-a (Chl-a) observations

Retrieval of Chl-*a* pigment from Aqua-MODIS involves two major steps: Atmospheric correction of visible bands (0.41–0.55 μm) measuring water leaving radiance (IOCCG, 2010) and development of suitable bio-optical algorithm measuring Chl-*a* concentration (O'Reilly et al., 2000). NASA's Ocean Biology Processing Group (OBPG) processes the global Level-0 Aqua-MODIS data in near-real-time mode and the datasets have been successively processed to Level-1A, Level-1B, Level-2, and Level-3 format. To avoid the data gaps in daily and weekly composites of Chl-*a* observations, we used level-3 monthly composites.

2.1.4. Primary productivity (PP)

Integrated mixed-layer primary productivity datasets (spatial resolution of ~9 km) for the period of January 2012, February 2010 and March 2009 were obtained from Goddard Space Flight Center (GSFC). After considering major input parameters from quality-controlled satellite observations, the estimation of primary productivity was carried out based on the Vertically Generalized Primary Production Model (VGPM) of Behrenfeld and Falkowski (1997).

2.1.5. Sea-ice extent

We used the sea-ice data set which was generated using the Defense Meteorological Satellite Program (DMSP) –F8-F17 Special Sensor Microwave Imagers (SSMIs) at a grid cell size of 25 km × 25 km (Cavalieri et al., 1996). The NASA Team algorithm developed by the Oceans and Ice Branch, Laboratory for Hydrospheric Processes at NASA Goddard Space Flight Center (GSFC) was used to generate the sea-ice product.

2.1.6. Sea level anomaly

The Merged Sea Level Anomaly (SLA) obtained from the AVISO live access server (http://atoll-motu.aviso.oceanobs.com) was used to study the sea level variability and the influence of mesoscale features in the study region.

2.2. In situ observations

Water sampling was carried out using a Seabird Conductivity–Temperature–Depth–Rosette system fitted with 10 L Niskin bottles. Conductivity was also measured using Autosal, and the difference between salinities measured by CTD and Autosal was within ± 0.1%. AWS anemometers were placed at a height of 10 m: